Stellar Abundances for the Galactic Archeology (SAGA) Database
— Compilation of the Characteristics of Known Extremely Metal-Poor Stars

Takuma SUDA,[1] Yutaka KATSUTA,[1] Shimako YAMADA,[1] Tamon SUWA,[2] Chikako ISHIZUKA,[1]

Yutaka KOMIYA,[3] Kazuo SORAI,[1] Masayuki AIKAWA,[4] and Masayuki Y. FUJIMOTO[1]

[1]*Department of Cosmosciences, Hokkaido University, Kita 10 Nishi 8, Kita-ku, Sapporo 060-0810*

[2]*Center for Computational Sciences, University of Tsukuba, Ten-nodai, 1-1-1, Tsukuba, Ibaraki 305-8577*

[3]*Department of Astronomy, Graduate School of Science, Tohoku University, Aramaki, Aoba-ku, Sendai 980-8578*

[4]*Hokkaido University OpenCourseWare, Hokkaido University, Kita 11 Nishi 5, Kita-ku, Sapporo 060-0811*

Abstract

We describe the construction of a database of extremely metal-poor (EMP) stars in the Galaxy. Our database contains detailed elemental abundances, reported equivalent widths, atmospheric parameters, photometry, and binarity status, compiled from papers in the literature that report on studies of EMP halo stars with $[\mathrm{Fe/H}] \leq -2.5$. The compilation procedures for this database were designed to assemble data effectively from electronic tables available from online journals. We have also developed a data retrieval system that enables data searches by various criteria and illustrations to explore relationships between stored variables. Currently, our sample includes 1212 unique stars (many of which are studied by more than one group) with more than 15000 individual reported elemental abundances, covering relevant papers published by 2007 December. We discuss the global characteristics of the present database, as revealed by the EMP stars observed to date. For stars with $[\mathrm{Fe/H}] \leq -2.5$, the number of giants with reported abundances is larger than that of dwarfs by a factor of two. The fraction of carbon-rich stars (among the sample for which the carbon abundance is reported) amounts to $\sim 30\%$ for $[\mathrm{Fe/H}] \leq -2.5$. We find that known binaries exhibit different distributions of the orbital period, according to whether they are giants or dwarfs, and also as a function of the metallicity, although the total sample of such stars is still quite small.

Key words: astronomical data bases: miscellaneous — stars: abundances — stars: evolution

1. Introduction

Extremely metal-poor (hereafter EMP, defined by $[\mathrm{Fe/H}] \leq -2.5$ in this paper) stars in the Galaxy carry information of the physical conditions in the early epochs when they were born, and are also unique probes of the production of elements by the first-generation stars when the Universe emerged from the so-called dark ages. Analyses of their kinematics also provide direct information on the early stages of galaxy formation (e.g., Carollo et al. 2007). The chemical compositions of these stars also impose constraints on the nucleosynthesis pathways involved with the formation of the elements throughout the early history of the Galaxy.

It is a long-standing problem as to whether one can identify the low-mass survivors of the first-generation (Population III) stars, those objects born from primordial clouds containing no elements heavier than lithium. If such stars did form, it remains possible that they could be found among the EMP stars, since there are processes (such as binary mass-transfer and/or the accretion of interstellar gas polluted by later generation stars) that could effectively "disguise" their true nature by making them appear more metal-rich at present.

Thanks to recent large-scale searches for candidate Very Metal-Poor stars [hereafter VMP, defined by $[\mathrm{Fe/H}] \leq -2.0$ according to the nomenclature of Beers and Christlieb (2005)], particularly by the HK survey (Beers et al. 1985, 1992) and by the Hamburg/ESO survey (Christlieb et al. 2008), the number of known VMP stars has increased dramatically since

the 1990s. Approximately ~ 1200 and ~ 1500 stars have been identified as being VMP to date, based on a medium-resolution spectroscopic follow-up of ~ 6000 and ~ 3600 candidates in the HK-I and HES surveys, respectively (Beers et al. 2005). This number is likely to expand quickly as additional VMP stars are identified from ongoing efforts, such as the Sloan Digital Sky Survey (in particular from SEGUE: Sloan Extension for Galactic Understanding and Exploration, see http://www.sdss.org). Furthermore, high-resolution spectroscopic observations with 8m-class telescopes, such as SUBARU, the VLT, and the KECK telescopes, are already beginning to elucidate the detailed abundance patterns of VMP stars.

Abundance analyses of EMP stars provide useful information about Galactic chemical evolution by comparing of their abundance patterns with those of more metal-rich stars with $[\mathrm{Fe/H}] \gtrsim -2.5$, including the globular cluster stars. At present, only three stars are known with metallicities well below $[\mathrm{Fe/H}] = -4$ (all of which have high-resolution abundance analyses available), while more than 100 stars are known with $[\mathrm{Fe/H}] < -3$, roughly half of which have detailed abundance analyses at present. A salient feature of EMP stars is the sharp cut-off below $[\mathrm{Fe/H}] \sim -3.5$ in the metallicity distribution function. Other important features of EMP stars are the large fraction of carbon-enhanced stars that are known to exist among them, especially below $[\mathrm{Fe/H}] \sim -2.5$ (Rossi et al. 1999), as well as the large scatter in the abundances of neutron-capture elements (Gilroy et al. 1988; McWilliam et al. 1995;

Ryan et al. 1996; François et al. 2007). The lighter elements, such as CNO, as well as the *p*- and *α*-capture elements and *s*-process elements, are used as tools to explore nucleosynthesis from H- and He-burning resulting from binary mass transfer affected by the evolution of low- and intermediate-mass AGB stars (Suda et al. 2004; Lucatello et al. 2006; Komiya et al. 2007). For heavier elements, the abundance patterns of individual EMP stars provide crucial information on the r-process elements produced (presumably) by individual supernova events (Truran 1981; Mathews & Cowan 1990). Such stars are also used as cosmo-chronometers for placing lower limits on the age of the Universe, based on determinations of the abundances of uranium and thorium (Sneden et al. 1996; Wanajo et al. 2002). A handful of stars that exhibit large enhancements of the r-process elements (Sneden et al. 1994; Hill et al. 2002; Frebel et al. 2007) have drawn the interest of researchers concerned with the nucleosynthesis processes in massive EMP stars, and the chemical evolution of the Galaxy. The determination of the isotopic abundances of ^{6}Li and ^{7}Li by high-resolution spectroscopy (Smith et al. 1993; Hobbs & Thorburn 1994; Asplund et al. 2006) also impacts observational constraints on Big Bang nucleosynthesis and the astrophysical origins of these elements.

In order to promote studies, such as those described above, and to make them more useful in aggregate (e.g., for statistical studies), it is desirable to construct a modern database of the elemental abundances (and other related properties) of metal-poor stars in our Galaxy. Although the available data on the abundances and properties of EMP stars has been greatly increasing in the past decades, thanks to the many high-resolution spectroscopic studies that have been conducted (Gilroy et al. 1988; Ryan et al. 1991; McWilliam et al. 1995; Ryan et al. 1996; Fulbright 2000; Preston & Sneden 2000; Burris et al. 2000; Mishenina & Kovtyukh 2001; Aoki et al. 2002; Cohen et al. 2002; Carretta et al. 2002; Johnson 2002; Nissen et al. 2002; Cayrel et al. 2004; Honda et al. 2004; Cohen et al. 2004; Simmerer et al. 2004; Spite et al. 2005; Barklem et al. 2005; Jonsell et al. 2005; Aoki et al. 2005; García Pérez & Primas 2006; Cohen et al. 2006; Aoki et al. 2007; François et al. 2007), there are no present databases that make these data readily available to astronomers and other researchers in order to conduct their own studies. Generally, it is quite difficult (particularly for the non-specialist) to collect the relevant quantities from the widely scattered literature. In part, this is because the data are presented in individual papers using wide varieties of formats, such as text, tables, and figures. Therefore, the compilation of pertinent information requires a great deal of human resources for individual investigators, who would greatly benefit from a more automated compilation.

To develop a more effective set of tools for compiling data for EMP stars, we have adopted a similar set of methodology for data compilation, developed by the Japanese nuclear data group[1] (Suda et al. 2006). We adopted the strategy of Hokkaido University Nuclear Reaction Data Center (JCPRG), which has developed tools for compilation via the internet, which alleviate much of the human resources required if the data were

input manually from the literature (Pronyaev et al. 2002). We differ from the JCPRG approach in that we have adopted a relational database management system for data storage (MySQL), rather than a text-based master database. We have also adopted their methods of utilizing the database through the internet by developing tools to retrieve data and draw summary graphs (Nouri et al. 2002; Otuka et al. 2005; Pritychenko et al. 2006).

In this paper, we describe the structure of the SAGA database, and present some results based on simple queries of the existing system. Our database enables queries of quantities such as the elemental abundances, photometry, atmospheric parameters, binarity, and position in the Galaxy, and the relationships between them. Thereby, we can begin to consider the characteristics of EMP stars in a statistical sense, and better draw global views of the nature of EMP stars in the Galaxy.

This paper is organized as follows. In section 2 we describe the compilation and retrieval system for our database. In section 3 we elaborate on the global characteristics of EMP stars in our sample. In section 4 we present a brief summary.

2. Overview of the Database and the Retrieval System

2.1. Characteristics of the SAGA Database

The SAGA database assembles available data for extremely metal-poor stars in the Galaxy from recent literature, and makes them available for observational and theoretical studies. At present, we have collected papers so as to cover a complete sample of metal-poor stars in the Galaxy with [Fe/H] ≤ −2.5, excluding stars in metal-poor Galactic globular clusters. At the same time, we compiled reference stars and stars with [Fe/H] > −2.5 listed in the same literature along with EMP stars. This metallicity range corresponds, theoretically, for evolved stars, to the occurrence of hydrogen-mixing into the helium convection zone during helium shell flash and the helium-flash driven deep-mixing episodes in the helium-burning region (Fujimoto et al. 2000), which plays a critical role in understanding the characteristics of EMP stars.

Thus far, we have compiled data for 1212 stars (based on 2243 independently reported measurements of stars, 1031 of which are included in multiple papers) from 121 papers published through 2007 December. Among them, the number of stars with [Fe/H] ≤ −2.5 amounts to 392, although it varies with the adoption of the derived iron abundance from multiple papers. The stellar parameters and abundance data that we have collected are based mostly on high-dispersion spectroscopy (typically $R \gtrsim 40000$), although some data obtained with lower dispersions are also included. We intensively gathered data from the latest papers, and currently trace back to 1995. We believe we have complete coverage for papers published from 2000 onward, except for a few redundant examples for which electronic data are only available on the Web.

The quantities compiled in the database are summarized in table 1. The data cover the stellar parameters and photometric data, as well as information gleaned from papers that included a log of observations. During the course of compilation, a unique entry number is assigned to each individual paper. Bibliographic data are identified by the title, authors, and reference code of the selected paper. The compiled data are stored as a table, following the example shown in table 1.

---

[1] The Stellar Abundances for Galactic Archeology database, SAGA. The database will be available at ⟨http://saga.sci.hokudai.ac.jp/⟩.

Table 1. Physical quantities compiled in the SAGA database.

Data table category	Item	Note
Bibliography	Title	
	Authors	
	Reference	
Observing log	Object name	
	Observing date	Including Julian date and universal time
	Telescope	
	Resolution	
	Typical S/N	
	Exposure	
	Radial velocity	
Position	RAJ(2000)	Right ascension (J2000.0)
	DEJ(2000)	Declination (J2000.0)
	l	Galactic longitude
	b	Galactic latitude
Abundances	[X/Fe]	Enhancement of element 'X' relative to iron
	[X/H]	Mass fraction of element 'X'
	$\log\epsilon$	$\log\epsilon_X \equiv \log(n_X) + 12$ where n_X is the number abundance of element 'X'
Atmosphere	$T_{\rm eff}$	Effective temperature
	$\log g$	Surface gravity
	[Fe/H]	Metallicity
	$v_{\rm turb}$	Velocity of microturbulence
Photometry	Magnitude	U, B, V, R, I, J, H, K
	Color index	$(B-V), (U-B), (V-R), (J-H), (H-K), (J-K), (V-K), (V-I),$
		$(R-I), \mathrm{E}(B-V)$
Equivalent width	EW	Equivalent width
	$\log\epsilon$	Line abundance
	$\log gf$	gf values
	χ	Excitation potential
Binarity	Binarity	Yes or No (unknown)
	Period	
	Radial velocity	
Solar Abundance	Reference	Adopted or assumed value(s)

The positions of the stars are obtained from the literature, the SIMBAD database, or the VizieR catalogues. Galactic coordinates are calculated, if required, and are also placed in the database. The data from the observing logs contain basic information concerning the observational set up that was employed, and may be used to obtain a quick review of individual stars. The records of (heliocentric) radial velocities are stored along with their dates of observation, which should prove to be useful for checking the status of the monitoring programs for binarity, as well as for use in studies of the space motions of the stars, when combined with the proper motions (some of which are presently available, and others that should become available in the future). We have compiled the adopted solar abundances from the literature, which enables us to evaluate the effect of using different solar abundances. If we remove this effect, we can obtain more homogeneous data for the relative abundances independent on the adopted solar abundances. The abundances of individual elements in our collected sample constitute more than 17000 records for species from lithium to uranium.

Figure 1 shows the number of stars that have available abundance data for each element, which clearly varies greatly, depending on the species considered. We distinguish abundance information based on fits to synthetic spectra of atomic and molecule lines from that based on equivalent-width measurements. These are stored as separate records. The data for reported isotopic abundances are also recorded separately in our database, although we have limited this information (for now) to the ratios $^{12}\mathrm{C}/^{13}\mathrm{C}$ and $^{6}\mathrm{Li}/^{7}\mathrm{Li}$. The stellar atmospheric parameters used to derive the spectroscopic abundances are available in most papers, and are compiled in the database. Photometric information (magnitudes and color indices), if available, is compiled from the literature. These are also useful for inspecting the stellar quantities, as discussed in the section 3. In particular, the V-band magnitude is used to obtain estimates of the distances to each star. The equivalent widths used by each analysis are compiled for the elements
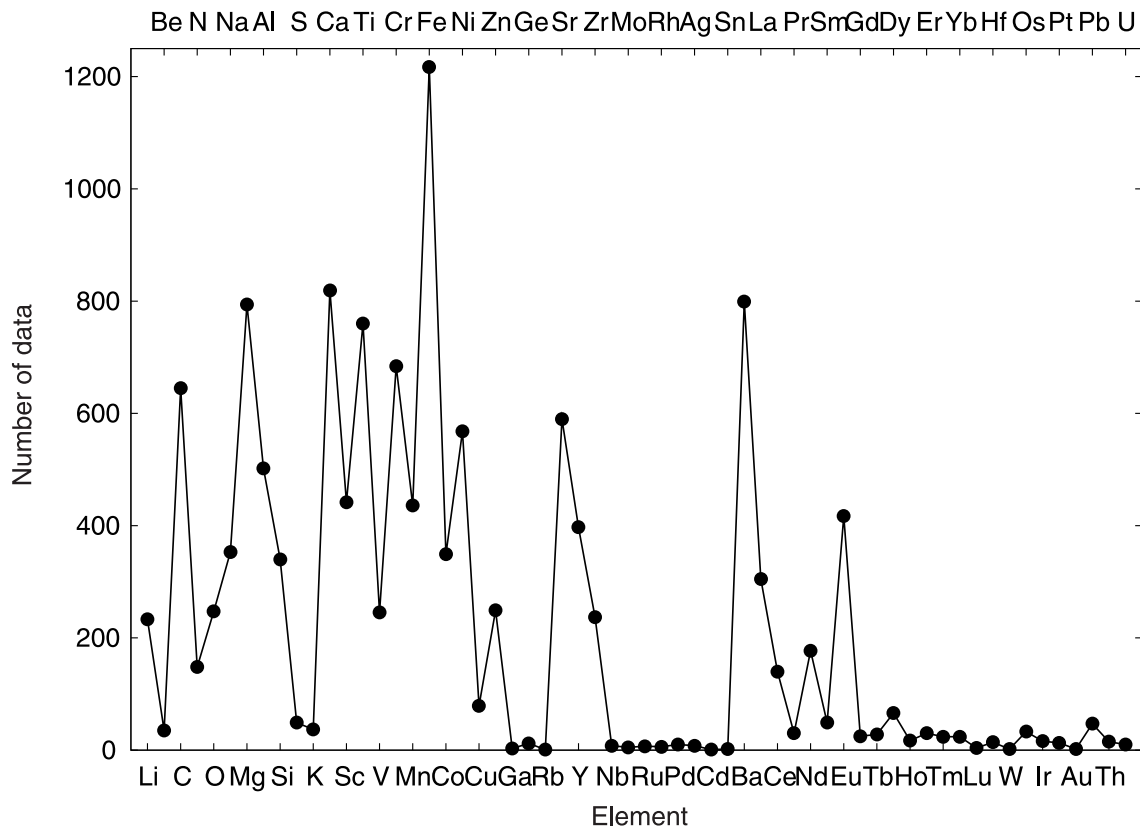
Fig. 1. Number of compiled data as a function of the chemical species.

and lines of each element, if available in the form of electronic data tables on the web. These could be used for re-analysis, if desired. The binary periods, as determined from the observed variations in radial velocities between observations obtained at different times, are compiled, although at present they are limited to a small number of systems. We plan to pay special attention to reported periods in future updates of the SAGA database, as information on the role that binary mass transfer may play on the observed surface abundances is thought to be a critical factor in identifying descendants of the first stars (Suda et al. 2004; Komiya et al. 2007).

We wish to remark on our treatment of the compiled object names. The name of a given star is one of the key identifiers for each record in the database, but it is not always unique. A few objects have several different names, according to the catalogues from which they were drawn. As pointed out by Beers et al. (1992), who referred to some HK survey stars as "multiple identifications", there are also cases in which the same catalogue duplicates a given object (due, for example, to overlapping regions of the sky being surveyed). The members of spectroscopic binaries are noted by the symbols "A" and "B", based on the notation employed in the original papers; the data are compiled separately for both members; only three such cases of binary stars with information for both members are present in the current database.

2.2. The Database Sub-Systems

The database consists of four sub-systems:(1) the reference management sub-system, (2) the data compilation sub-system,

(3) the data registration sub-system, and (4) the data retrieval sub-system. The first three sub-systems are used to compile and verify the observational data from the literature, while the last one is for use of the database. These sub-systems are described briefly below.

2.2.1. Reference management sub-system

The reference is listed, based on a search of the papers conducted with the Astrophysics Data System (ADS) Abstract Services,[2] which report on observations of metal-poor stars. We then check the candidate papers to see whether they have included the required information, such as the results of abundance analyses conducted at sufficiently high spectral resolving power. At present, we have endeavored to collect papers that report stars with [Fe/H] < -2.5. We intend to increase the upper abundance limit in future updates of SAGA. For the papers that pass these requirements, a unique reference code is registered on the web system. Most of the papers added to the list are assembled by the data compilation sub-system, except when the required data are not available. The data are collected for all stars that are contained in the papers, including those stars with higher reported metallicities.

2.2.2. Data compilation sub-system

The observational data are taken from each paper accepted by the reference management sub-system, and stored as comma separated values (CSV) files. The data compilation sub-system enables a set of data editing routines to input data easily by copying it electronically. Human data editors pick up the

---

[2] ⟨http://adsabs.harvard.edu/abstract_service.html⟩.

required data (listed in table 1) from the papers by using an interface appropriately tailored for the targets of the compilation. For example, when data editors store the data from the numerical data table, they use the interface to convert the data table into CSV files. The data table converter can deal with many types of electronic data table formats available online, which differ from paper to paper as well as from journal to journal. We define each set of data files of the abundances and stellar parameters for a given reference and object; the reference and object name are the primary keys of the database.

2.2.3. Data registration sub-system

The stored CSV data files are registered into the database server through using the data registration sub-system run by the SAGA database administrator. We have adopted the publicly available relational database management system MySQL. During the registration process, we convert the stored data into several additional useful outputs for the data retrieval sub-system described below. For example, the abundance data, given in units of [X/Fe], $\log \epsilon$, or [X/H] from each paper, are converted into each other with the use of solar abundance data. For now, we have adopted the solar abundances of Grevesse et al. (1996). For example, the quantity [X/H] (where X corresponds to the species under consideration) is computed from $\log \epsilon$ automatically in the registration script as [X/H] = $\log \epsilon(X) - \log \epsilon(X, \odot)$.

At the same time, HTML files that include the original information on the objects in the literature, and summary figures of the abundance distribution for individual elements, are generated for each object. These files can be used to obtain a quick review of the data included in each paper, or for each object, so that users can trace the links to the data files and abundance distributions for stars in the database, and easily access the information on the paper(s) from which they were drawn.

2.2.4. Data retrieval sub-system

We constructed a web-based data retrieval sub-system for EMP stars based on a script written in Perl/CGI. Users can access and select data based on various criteria, and then inspect the selected data on a diagram with user-specified axes. A screen snapshot of the query form is shown in figure 2. The first section of the form is used to specify the quantities to draw in the graph, the axes in the first three lines, and the criteria for object selection in the additional lines. One can choose any desired quantity among those listed in table 1 to plot, e.g., the abundances of any elements (in any units of [X/Fe], [X/H], and $\log \epsilon$), the atmospheric parameters, the photometric bands, the binary periods, and also the stellar position and distance from the Sun estimated from the observed data. In the first column, various categories of data can be chosen as axes. In the second and third columns, one can specify the quantity to be plotted. In the third column, one can specify the quantity directly by, for example, setting the form input to "[Fe/H]". For elemental abundance data, it is also possible to define new quantities beyond those listed in the original papers. For example, users can obtain abundance ratios, such as [Ba/Eu] or [(C+N)/Fe], or even [(Pb+Ba)/C], whose values and errors are calculated internally from the corresponding data. The 4th and 5th columns set the range of the values for each selected quantity, with the option in the 6th column of whether to include or exclude the objects that have data with only an upper

limit reported. In the 4th line, users can specify the required range in the data, if necessary, to select or remove the objects from plotting, e.g., by setting $+0.5 \leq$ [C/Fe] $\leq +2.0$. The number of criteria can be extended to as many as desired by the user. In the second section of the form, one can set any additional criteria desired, such as the object name, binarity status and reported period, photometric magnitude in any bands, and the resolving power of the observational setups used. The third section specifies the bibliographic criteria. Through the use of these retrieval options, users can extract the data containing a specific object name, author, and the range of the year of publication. Retrieval options are set in the fourth section, such as the number of data to display in the resulting list and order of the list. By selecting the output option, it is possible to obtain the distribution of the quantities in the form of a histogram with an arbitrary size of bin width and range.

Cross-matched retrieval and plots are also possible as an option, which allows for the extraction of data from different papers. This might be used for checking the relationships between parameters when the object name is common between several papers, but its data are not. Users should bear in mind that the reliability of the results may be degraded due to the difference in the observational setups used by the individual observations.

A screen snapshot of an example retrieved set of records is shown in figure 3. The retrieved records from the MySQL server are displayed in table format on the browser. The columns represent, from left to right, the checkbox to select data to be plotted, the object name, the reference code of the paper, the values of [Fe/H], $T_{\rm eff}$, and $\log g$, as well as the values for the quantities selected as the axes of the plotted diagram. The data to be plotted can be selected by the radio buttons that are set initially based on the criterion, such as the published year of derived data, the adopted lines for element species, and the size of data errors. By using the provided links to the object names and reference codes, one can trace the information on object and reference, respectively. For selected data, the diagram is drawn in the web browser according to the choice of options, using the publicly available graphic software Gnuplot. By specifying the appropriate plotting option, users can plot the selected data sets from two or more papers that match the selection criteria for each object. Graphs drawn in the browser are equipped with simple functions for editing. The standard options are to change the labels, the legends, and the scales and ranges of the graph. Automatic links to the information on objects are generated in all data points on the graph. Users can also download the figures in various formats (png, eps, ps, and pdf, in color or in black and white), and can download the data from the form to their local computer. Plotted numerical data, as well as the script to reproduce the figure plotted are available from the server, if one wishes to edit the graph in more detail. Numerical data are also accessible by tracing the link to each data set in the list.

It should be noted that we temporarily use a single data set for a given element from one paper in the data-retrieval system, and preferably adopt 1D LTE abundance. Therefore, we adopt only one element abundance for a single object for plural element abundances, such as different ionization status, while we compile all data for any kinds of ioniazation status

Data Retrieval System for SAGA Database

Last update of database: 2008-08-06 12:02:40

Query

	search example reset

Graph Options							
Xaxis	Category ▾	any ▾	[Fe/H]	From :	To :	Include ▾	data with upper limit
Yaxis	[X/Fe] ▾	C ▾		From :	To :	Include ▾	data with upper limit
Criterion ⊞	Category ▾	any ▾		From :	To :	Include ▾	data with upper limit

Optional Criterion	
Object	[_____] ex) "HE0107-5240", "CS", "0107"
Binarity	☐ Binary Nature Period (days) : From [____] To [____]
Magnitude	Band ▾ : From [____] To [____] mag
Resolution	[____] < R < [____]

Bibliographical Criterion	
Author	[_____] First author ▾ ex) "Lastname" ⦿ strict ○ forward agreement ○ backward agreement ○ fuzzy
Reference	ALL ▾
Publication Year	From [____] To [____]

Retrieval Options	
Display / Page	10 ▾
Order by	Object ▾
Output Option	single file ▾
Histogram Option	Bin Width [____] Range [____] [____] (necessary for histgram)
Cross Search	Retrieve data across papers ▾
	search example reset

Fig. 2. Screen snapshot of the top page of the data-retrieval sub-system for the SAGA database.

and molecular lines. In the current system, we prefer to adopt a lower ionization state, i.e., the [Fe I/H] abundance is adopted in plotting the viewgraph if the [Fe I/H] and [Fe II/H] abundances are available in the database. For atomic and molecular lines, we currently adopt the C II, CN, and O I abundance, rather than the CH, NH, and OH abundance for carbon, nitrogen, and oxygen abundance, respectively. This may sometimes cause inconvenience, but the users can choose one of the adopted abundances for the selected paper and object. Of course, users can check the element abundances with different lines by the quick review files of the database stated above, and by the original papers linked to them.

3. Global Characteristics of Known EMP Stars Studied at High Spectral Resolving Power

In this section we discuss the basic properties of the EMP stars in the SAGA database. Here, we focus on the characteristics of the sample stars as a whole, and defer any detailed analyses of the elemental abundances of individual stars, and any discussion of insight gained from them, to subsequent papers. All of the figures presented below were obtained by use of the data-retrieval sub-system. For those objects with multiple sources of data, the values plotted were adopted from the most recent papers.

Figure 4 shows the locations of the sample stars in an effective temperature vs. surface gravity diagram. There are 1110 stars with these stellar parameters measured from among the 1212 stars currently registered in the SAGA database. In our

system, the objects were classified according to the evolutionary stage and their iron and carbon abundances. For convenience of the present discussion, we adopted the following conventions. The objects were classified into dwarfs and giants (labeled "MS" and "RGB", respectively), according to the requirement that giants have $T_{\mathrm{eff}} \leq 6000\,\mathrm{K}$ and $\log g \leq 3.5$. We set the boundary between the EMP star (labeled "EMP") and the other population II stars at $\mathrm{[Fe/H]} = -2.5$, which is based on stellar-evolution models for low- and intermediate-mass in which proton mixing driven by helium burning occurs for $\mathrm{[Fe/H]} \lesssim -2.5$ (Fujimoto et al. 2000; Suda et al. 2004). We also consider those stars with $\mathrm{[C/Fe]} \geq +0.5$ as "CEMP" and "C-rich" according to the metallicity $\mathrm{[Fe/H]} \leq -2.5$ and > -2.5, respectively. It should be noted that the criterion of carbon enrichment is different from that in Beers and Christlieb (2005), who defined $\mathrm{[C/Fe]} \geq +1.0$. Accordingly, we have seven classes of objects, i.e., "CEMP RGB", "CEMP MS", "EMP RGB", "EMP MS", "C-rich RGB", "C-rich MS", and "MP"; the last label "MP" denotes the other metal-poor stars that are neither classified as "EMP" nor "C-rich", irrespective of their status as "RGB" or "MS".

Among the sample stars, EMP stars fall mostly in the range of $4500 < T_{\mathrm{eff}} < 6500\,\mathrm{K}$, which is significantly narrower than the range covered by the more metal-rich stars. This is due to observational bias in the selection of targets for high-resolution spectroscopy, as researchers have naturally favored studies of the most extreme stars in the past decade. In figure 4, theoretical evolutionary tracks are plotted for a model star of $0.8 M_{\odot}$ and $\mathrm{[Fe/H]} = -2.3$. The EMP stars occupy the

Search Result

plot | restart | reset | plot_all
Results : 615

#	○	Object	Reference	[Fe/H]	Teff	logg	[Fe/H]	[C/Fe]
1	□	CS22942-019	W.Aoki+,ApJ, 580, 1149, 2002	-2.64	5000	2.4	○ -2.64	
			W.Aoki+,, 54, 933, 2002	-2.64	5000	2.4	⊙ -2.64	⊙ 2
			G.W.Preston+,AJ, 122, 1545, 2001	-2.67	4900	1.8	○ -2.67	⊙ 2.2
2	□	CS22944-032	D.K.Lai+,AJ, 128, 2402, 2004		5528	3.44	○ -2.64	
			D.K.Lai+,ApJ, 667, 1185, 2007	-2.64	5528	3.44	⊙ -2.64	⊙ 0.65
3	□	CS22945-024	J.A.Johnson+,ApJ, 658, 1203, 2007	-2.26	5289	3.04	⊙ -2.26	⊙ 0.7
4	□	CS22945-028	P.S.Barklem+,AAP, 439, 129, 2005	-2.66	5126	2.55	⊙ -2.66	⊙ 0.21
5	□	CS22947-187	A.McWilliam+,AJ, 109, 2757, 1995	-2.6	5160	1.3	○ -2.49	○ 1.03
			J.A.Johnson+,ApJ, 658, 1203, 2007	-2.25	5489	3.44	⊙ -2.25	⊙ 0.6
6	□	CS22948-027	W.Aoki+,ApJ, 567, 1166, 2002	-2.57	4600	1	○ -2.56	○ 2
			V.Hill+,AAP, 353, 557, 2000	-2.47	4800	1.8	○ -2.47	○ 1.9
			B.Barbuy+,AAP, 429, 1031, 2005	-2.47	4800	1.8	○ -2.47	○ 2.43
			G.W.Preston+,AJ, 122, 1545, 2001	-2.6	4600	0.8	○ -2.79	○ 2.1
			W.Aoki+,ApJ, 655, 492, 2007	-2.3	5000	1.9	⊙ -2.21	⊙ 2.12
7	□	CS22948-066	R.Cayrel+,AAP, 416, 1117, 2004	-3.14	5100	1.8	○ -3.13	○ -0.02
			M.Spite+,AAP, 430, 655, 2005	-3.14	5100	1.8	○ -3.14	○ 0
			A.McWilliam+,AJ, 109, 2757, 1995	-3.1	5020	1.45	○ -3.03	○ -0.5
			M.Spite+,AAP, 455, 291, 2006	-3.14	5100	1.8	○ -3.14	○ 0.08
			S.M.Andrievsky+,AAP, 464, 1081, 2007	-3.14	5100	1.8	⊙ -3.14	
8	□	CS22948-104	J.A.Johnson+,ApJ, 658, 1203, 2007	-2.39	5270	2.99	⊙ -2.39	⊙ 0.25
9	□	CS22949-008	J.A.Johnson+,ApJ, 658, 1203, 2007	-1.92	6144	3.82	⊙ -1.92	⊙ 1.15
10	□	CS22949-029	D.K.Lai+,AJ, 128, 2402, 2004		6244	3.81	○ -1.7	
			D.K.Lai+,ApJ, 667, 1185, 2007	-1.7	6244	3.81	⊙ -1.7	⊙ 0.55

previous | next

1 2 3 4 5 6 7 8 9 10 **11** 12 13 14 15 16 17 18 19 20
21 22 23 24 25 26 27 28 29 30 31 32 33 34 35 36 37 38 39 40
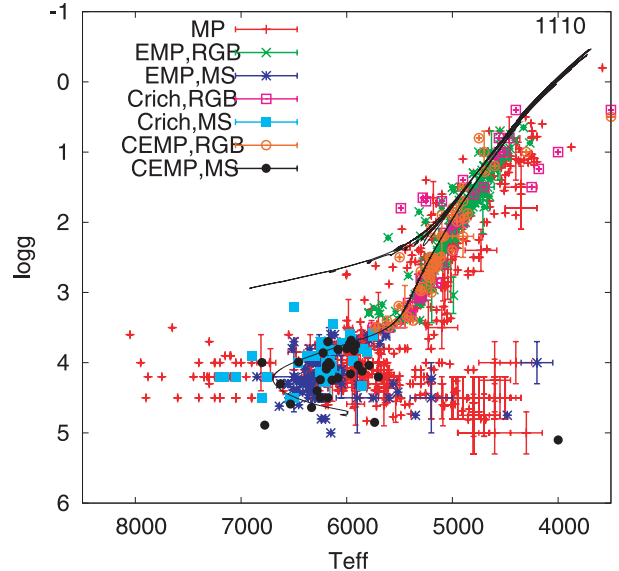41 42 43 44 45 46 47 48 49 50 51 52 53 54 55 56 57 58 59 60
61 62
PAGE : 11 / 62

Fig. 3. Screen snapshot of the search result of the data retrieval sub-system of the SAGA database. In this case, the X-axis and Y-axis are set to [Fe/H] and [C/Fe], respectively.

Fig. 4. Distribution of SAGA database stars in the $T_{\rm eff}$ vs. $\log g$ diagram, as plotted by the data-retrieval sub-system. $T_{\rm eff}$ and $\log g$ are taken from the atmospheric parameters adopted in the original papers. A stellar evolutionary track for a model with $0.8 M_\odot$ and $[{\rm Fe/H}] = -2.3$ is superposed for a comparison. The number in the top-right corner denotes the number of sample stars included in the plot. The legend indicates our adopted classifications according to the evolutionary status and abundance characteristics. Details are provided in the text.

evolutionary track near the main-sequence turnoff and on the lower giant branch. The dearth of sample stars below $T \simeq 4500\,$K, including near the tip of the RGB, is related to a difficulty in obtaining abundance information for many elements due to the presence of strong molecular features. One exception is the dwarf G 77–61, with $T_{\rm eff} = 4000\,$K, according to Plez and Cohen (2005), who revised the metallicity from the value $[{\rm Fe/H}] = -5.6$ assigned by Gass et al. (1988) to $[{\rm Fe/H}] = -4.01$. Stars on the AGB are also scarce among EMP stars, other than CS 30322−023 (Masseron et al. 2006, with $[{\rm Fe/H}] = -3.5$ and $T_{\rm eff} = 4100$K). At higher temperatures, our sample of EMP stars lacks blue stragglers beyond the turnoff, while they are abundant among the more metal-rich sample stars. In addition, the horizontal-branch stars with temperatures $T_{\rm eff} \gtrsim 5500\,$K are absent in figure 4, again attributable to the selection bias associated with follow-up observations. Such stars have not been studied in great detail at high resolution, even though targets exist, e.g., from Beers et al. (1992). At low metallicity, stars of higher temperature do not display a wide range of detectable absorption features associated with heavier elemental species, so they are understandably not preferentially chosen for a high-resolution follow-up.

Figure 5 shows the metallicity distribution for the 1205 sample stars[3] with available iron abundance measurements. The distribution peaks near $[{\rm Fe/H}] \simeq -2.7$; the decrease of sample stars at higher metallicity is an artifact of
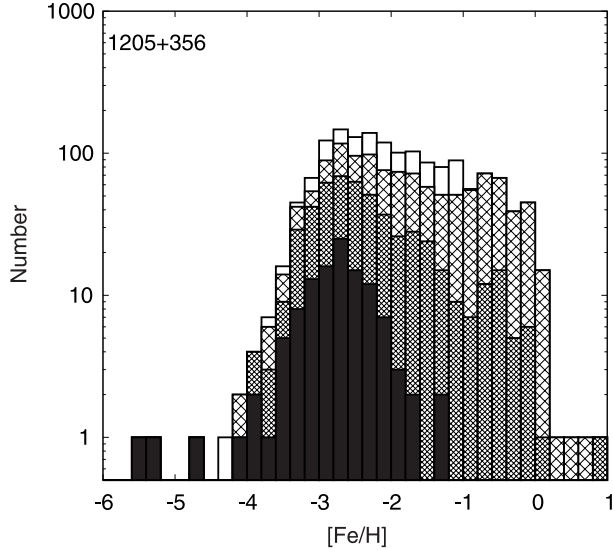
selection effects. Since a confident assignment of metallicity for stars with $[{\rm Fe/H}] < -3$ can only be determined from high-resolution spectroscopy, a general tendency exists for a decreasing number of metal-poor stars at lower metallicity. The sharp drop discernible for $[{\rm Fe/H}] < -4$ reflects the metallicity distribution function of field halo stars identified to date; only 5 stars are found below this metallicity (including HE 0557−4840, with $[{\rm Fe/H}] = -4.8$, discovered by Norris et al. (2007), and two stars very close to the boundary, CD-38°245 with $[{\rm Fe/H}] = -4.2$, and G 77-61 with $[{\rm Fe/H}] = -4.03$), while $\simeq 150$ stars are known with metallicities in the range $-4 < [{\rm Fe/H}] < -3$. In this figure, we have included medium-resolution follow-up observations of "saturated stars" $(9 < B < 14)$ from the HES provided by Frebel et al. (2006), and the cooler, carbon-rich stars from the HERES data sample of Lucatello et al. (2006). The inclusion of these data, denoted by open boxes, increases the apparent steepness of the metallicity distribution function at $[{\rm Fe/H}] \gtrsim -4$. Note that the data from these authors lack some of the information on the stellar parameters; these samples are excluded in the following discussion.

In figure 6 we show the V-magnitude distribution of the 866 stars included in the SAGA database. It exhibits a bimodal distribution, with two peaks at $V \simeq 8$–9 and 13–14, which reflects the history of past survey efforts. Stars in the brighter peak are primarily those discovered by Bond (1980), with a limiting magnitude of $B \simeq 10.5$, and from the high-velocity star survey (Carney & Peterson 1981) and Carney et al. (1994). The deficiency of stars in the spectroscopic sample with apparent magnitudes in the range $9 \lesssim V \lesssim 13$ is due to
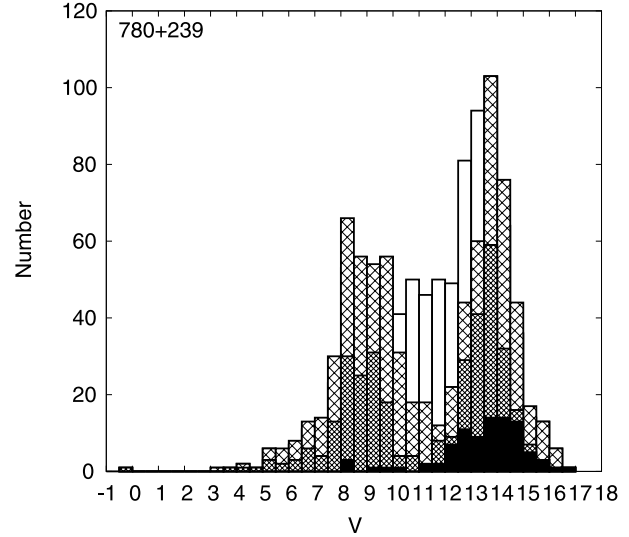
---

[3] The present database does not include iron abundance for 7 stars because it is not given in the original paper.

Fig. 5. Metallicity distribution ([Fe/H]) for stars currently registered in the SAGA database. A total of 1205 stars with measured iron abundances, denoted by hatched boxes, are divided into three groups: C-rich stars defined by [C/Fe] > +0.5 (filled boxes), giants defined by $T_{\rm eff} < 6000\,{\rm K}$ and $\log g < 3.5$ (shaded boxes), and an additional 347 stars from the bright metal-poor sample (Frebel et al. 2006) and the C-rich sample in Lucatello et al. (2006) (open boxes). Group classifications are not taken into account for these latter samples.

Fig. 6. Distribution of the V-magnitudes for stars in the current SAGA database. There are 866 stars in our sample with known V-magnitudes. The meanings of the boxes are the same as in figure 5, but the stars from Lucatello et al. (2006) are not included. The brightest star is HD 124897, which has $V = -0.05$. For the 239 bright metal-poor sample of Frebel et al. (2006), V-band magnitudes are computed from the B-magnitudes and (B−V) colors available in the literature.

an observational bias in later objective-prism surveys. The HK survey and the HES are designed to search in the ranges of $12 < B < 15.5$ (Beers et al. 1985) and $14 < B < 17.5$ (Christlieb et al. 2001b). The apparent dominance of dwarfs in between the two peaks can be explained by the sampling of high-velocity stars in this range, since stars with high proper motions are found almost exclusively among dwarfs. For the bright ($B < 14$) stars on the HES plates, the data recovery is now ongoing (Frebel et al. 2006). The 286 stars observed with medium-resolution follow-up spectroscopy to date partially fill the gap around $V \sim 11$.

In the metallicity range $[{\rm Fe/H}] < -2.5$, our sample consists of a total of 369 EMP stars, which contains 253 giants and 116 dwarfs. Among them, there are 81 C-rich stars (51 giants + 30 dwarfs). Komiya et al. (2007) theoretically approximated the fraction of dwarfs (and subgiants, using the definition of $\log g \geq 3.5$), relative to giants, to be $\sim 40\%$ for a limiting magnitude of 15 mag. This is in contrast to the flux-limited sample, with a limiting magnitude of 15.5 mag from Beers et al. (1992), whose data show that approximately two-thirds of their sample are turn-off stars (due to a known temperature-related selection bias). In the SAGA database, among the stars with $V \leq 15.5$, dwarfs represent 54% of the total.

Previous work (e.g., Lucatello et al. 2006) has claimed that CEMP stars occupy $\sim 20\%$ of EMP stars. Note that the fraction of C-rich stars can be as large as $\sim 30\%$, if we take the number of stars with carbon detection as a denominator, instead of the total number of EMP stars. Note that many previous workers have adopted a more conservative definition ([C/Fe] > +1.0) for the identification of CEMP stars than we use in our present discussion ([C/Fe] > +0.5). Figure 6 shows a large fraction of

C-rich stars in the SAGA datbase for $V \gtrsim 12$. Even though this is surely influenced by a variety of selection biases, the discoveries of the so-called ultra ($[{\rm Fe/H}] < -4.0$) and hyper ($[{\rm Fe/H}] < -5.0$) metal-poor stars, all of which exhibit large carbon enhancements, suggests that the fraction of CEMP stars is quite high at the lowest metallicities. It should be stressed that the observed fraction is unlikely to be biased at metallicities of $[{\rm Fe/H}] \lesssim -3.0$, because of a difficulty in predicting abundances with medium-resolution spectroscopy in this regime. In any case, our present sample confirms that the fraction of carbon-rich stars is larger at lower metallicity. In the current SAGA database, for $V \lesssim 10$, there are few stars with $[{\rm Fe/H}] \sim -3$, and no stars with $[{\rm Fe/H}] < -3.5$ (see figure 7).

According to our selection criteria for assembling EMP stars from published papers, the total fraction of carbon-rich stars ($[{\rm C/Fe}] \geq +0.5$) is 13.4% (24.1% among stars with derived carbon abundance). Among them, C-rich EMP stars ($[{\rm Fe/H}] \leq -2.5$) comprise 22.0% (28.6%) of the total sample of EMP stars. In particular, C-rich EMP giants occupy 20.2% (21.4%) of EMP stars, while C-rich EMP dwarfs represent 25.9% (66.7%). The extreme discrepancy of the C-rich fraction among the C-detected sub-sample is also found for the entire sample (20.4% for giants and 33.7% for dwarfs), and is due to the sensitive dependence of the detection limit on [C/H] for increasing effective temperatures [see figure 11 of Aoki et al. (2007)]. Even if we change the criteria on metallicity and carbon enhancement to $[{\rm Fe/H}] \leq -3.0$ and $[{\rm C/Fe}] \geq +1.0$, a similar trend is obtained [16.8% (21.4%) in total, 16.3% (16.9%) for giants, and 18.2% (66.7%) for dwarfs], although the sample size becomes small [125 (98) stars with $[{\rm Fe/H}] \leq -3.0$]. These two fractions for different criteria may possibly give the lower and upper limits for the true C-rich fraction. These values may be ascribed to the motivations of observers,
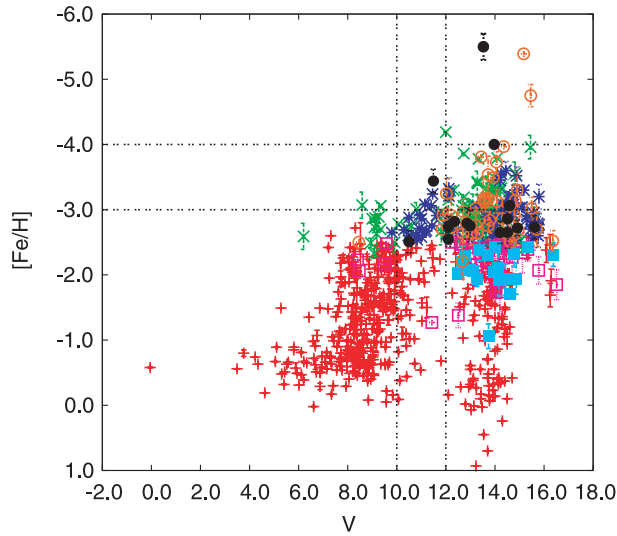
Fig. 7. Relationship between the metallicity and V-magnitude in 767 sample stars. The meanings of the symbols are the same as in figure 4.
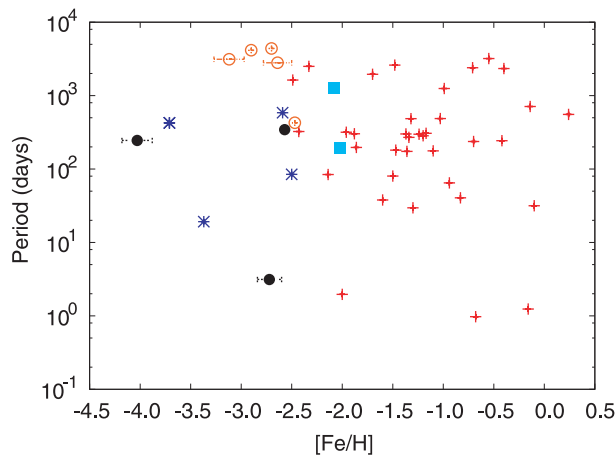

Fig. 8. Binary period distribution of the 51 stars with measured periods in the SAGA database. The meanings of the symbols are the same as in figure 4.

i.e., observers may have specifically intended to detect carbon in order to investigate the characteristics of C-enhanced stars. Accordingly, the C-rich fraction among the total sample has been increased by re-investigations of the known C-enhanced sample. On the other hand, C-rich features can be seen in the initial low- to intermediate-resolution spectra, selected from, for example, Christlieb et al. (2001a), which may argue that the current C-rich fraction among C-detected samples in the SAGA database may be a reasonable approximation of reality.

There are 51 known binaries present in the SAGA database. This is a surprisingly small value (less than 10% of the total sample), when we consider the large binary fraction ($\sim 50\%$) among nearby stars of younger populations. One of the primary reasons is the small number of EMP stars that have received attention from velocity monitoring programs during the past decade (and the short span in time of monitoring programs for those that have). Another reason could be that EMP stars

may include a large fraction of long-period binaries, and the resulting difficulty in detecting changes in their observed radial velocities. It has been suggested by Komiya et al. (2007), from the standpoint of stellar evolution, that most EMP stars were born as low-mass members of binary systems, and only those with large orbital separations could have survived the mass-transfer event when the primary stars swelled at the end of their lives. Observationally, it has also been reported by Preston and Sneden (2000) that C-rich stars among the sample of blue metal-poor stars exhibit longer periods than those of their C-normal counterparts. Binary periods have been estimated for 51 stars in the SAGA database, and range from ~ 1 to ~ 4000 d. The distribution of periods is shown in figure 8 as a function of the metallicity. Although the sample is very small, it clearly shows a difference in the observed binary periods between giants and dwarfs, with giants having systematically longer periods than dwarfs. Interestingly, there are 4 CEMP giants with long periods, in excess of $P > 2500$ d, while 7 EMP and CEMP dwarfs occupy the region with $P < 1000$ d. The lack of short-period binaries for giants could be understood in terms of their larger radii by supposing that the binary separations must be larger than the radius of the giants. On the other hand, the lack of long-period binaries for dwarfs may possibly be attributed to the length of time they have been monitored, which should be improved in the future. For stars with $[Fe/H] > -2.5$, some blue metal-poor stars show long periods of > 1000 d. Since, as argued in Komiya et al. (2007), binaries may have played an important role in the early epochs of the Galaxy, much more data on the binarity and period distributions are desired.

The spatial distribution for 708 stars from the SAGA database is shown in figure 9. The distance is computed from the V-band and the stellar luminosity, the latter of which was derived from the effective temperature and the surface gravity of the model atmosphere by assuming a stellar mass of $0.8M_\odot$. The coordinates were taken from the literature or from the SIMBAD database. In some cases, the Galactic coordinates were computed from the equatorial coordinates. The plotted sample includes 203 EMP stars. Among them, only 36 and 14 stars are CEMP giants and CEMP dwarfs, respectively. The maximum distance to the dwarfs is estimated to be ≈ 5 kpc from the Sun, while the maximum distance is ≈ 28 kpc for giants.

4. Summary and Discussion

We have constructed the SAGA (Stellar Abundances for Galactic Archeology) database of extremely metal-poor stars in our Galaxy. The compiled data are accessible on the web, and are presenting open to all researchers. Our database includes information on observational details, abundances, atmospheric parameters, photometry, equivalent widths, and binarity status and periods. These data are taken from published papers, with the use of a web-based system of data compilation equipped with useful tools to convert them from various forms of electronic data tables into the CSV format. A data retrieval system has been developed that enables the retrieval and plotting of data selected according to various criteria.

Our sample includes 1212 stars with distinct object names,
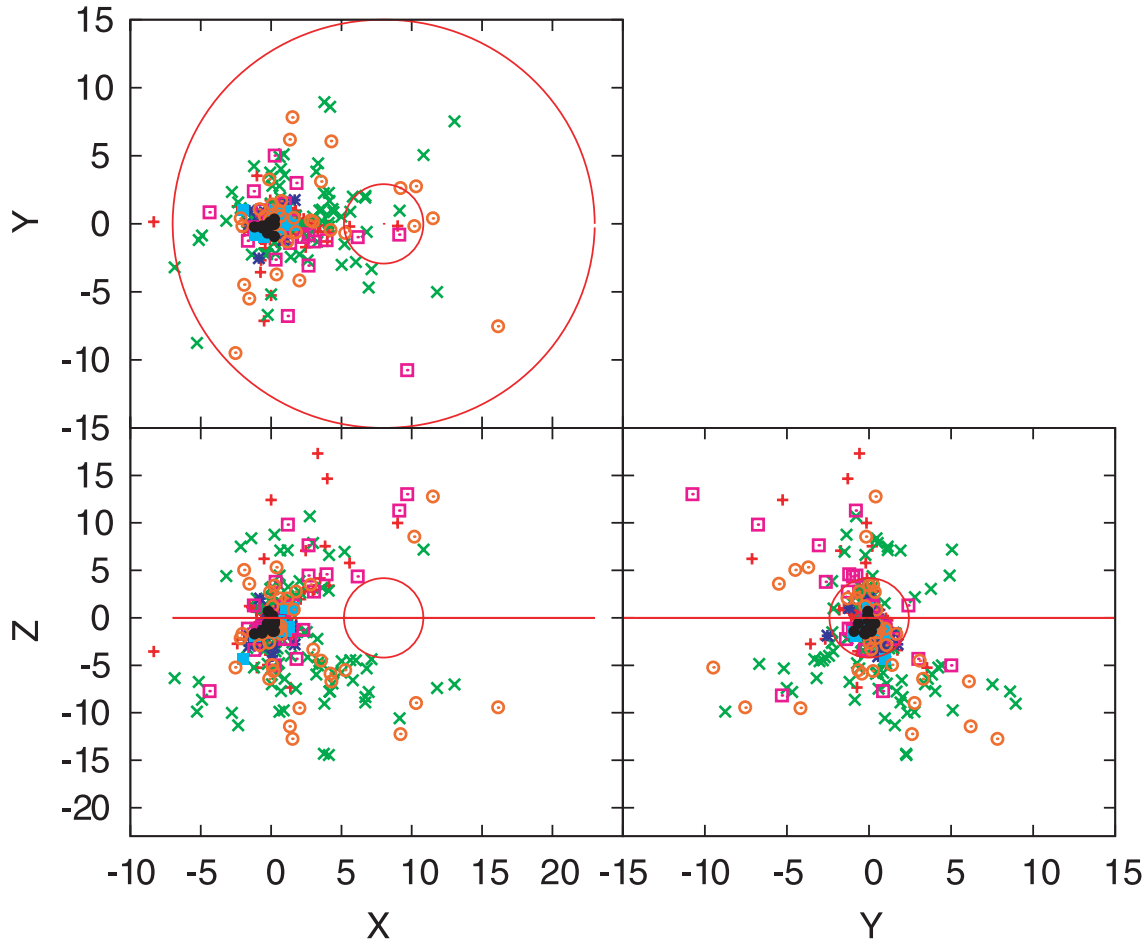
Fig. 9. Spatial distribution of 708 stars from the SAGA database. The distances to stars were estimated by assuming that all stars have $0.8M_\odot$. The coordinates X, Y, Z are set at the local standard of rest, and are directed to the Galactic center, counter-rotation direction, and north Galactic pole, respectively. The Galactic disk and center are also schematically shown by lines and circles. The meanings of the symbols are the same as in figure 4.

roughly half of which are giants. The number of giants becomes twice as large as that of dwarfs if we consider only stars with [Fe/H] < −2.5. The fraction of carbon-enhanced stars ([C/Fe] ≥ +0.5) amounts to ∼ 30% among the sample of stars with derived carbon abundance for [Fe/H] < −2.5. The sample stars exhibit a bimodal distribution of V-band magnitudes, which is ascribed to the different coverage of the effective magnitude range among the large-scale surveys of metal-poor stars. There may exist different distributions of binary periods among the stars with this information available. It is shown for stars with [Fe/H] ≲ −2.5 that those binaries with a giant member have typically longer periods than those with a dwarf member, and that there are no dwarfs in binaries having periods of > 1000 d yet confirmed. Considering the spatial distribution, our sample may have some biases for discussing the properties of metal-poor stars because of the different sampling volumes for dwarfs and giants. In fact, we only have detailed elemental abundances for dwarfs within ≲ 5 kpc from the Sun, while giants cover distances extending to more than ≳ 20 kpc in the current sample.

Since the EMP stars in our Galaxy are useful probes for our understanding of the chemical and formation history of

our Galaxy, large increases in such data are desired by both observational and theoretical reseaches. A number of observing projects are planned to increase the stellar sample. For example, the stellar extension program of the Sloan Digital Sky Survey, SDSS/SEGUE, is obtaining medium-resolution spectra from which additional EMP stars may be selected to a depth of up to ∼ 100 kpc (Beers et al. 2004). LAMOST (Zhao et al. 2006) is a multi-fiber 4 m telescope project that will enable up to 4000 stellar spectra to be obtained simultaneously in each exposure. The total survey effort is planned to encompass several million stars. These projects will increase the number of candidate EMP stars by several orders of magnitude in the near future, as compared with the number of known EMP stars at present. A high-resolution spectroscopic follow-up will be required, which will make use of dedicated programs, such as the proposed WFMOS effort on the Subaru telescope, and with the next generations of Extremely Large Telescopes, with diameters of 30 m or more.

It is important for us to understand how large are the discrepancies caused by independent analyses. In order to check the difference among the derived abundances by different authors, we picked up 17 stars from our sample, and compared their
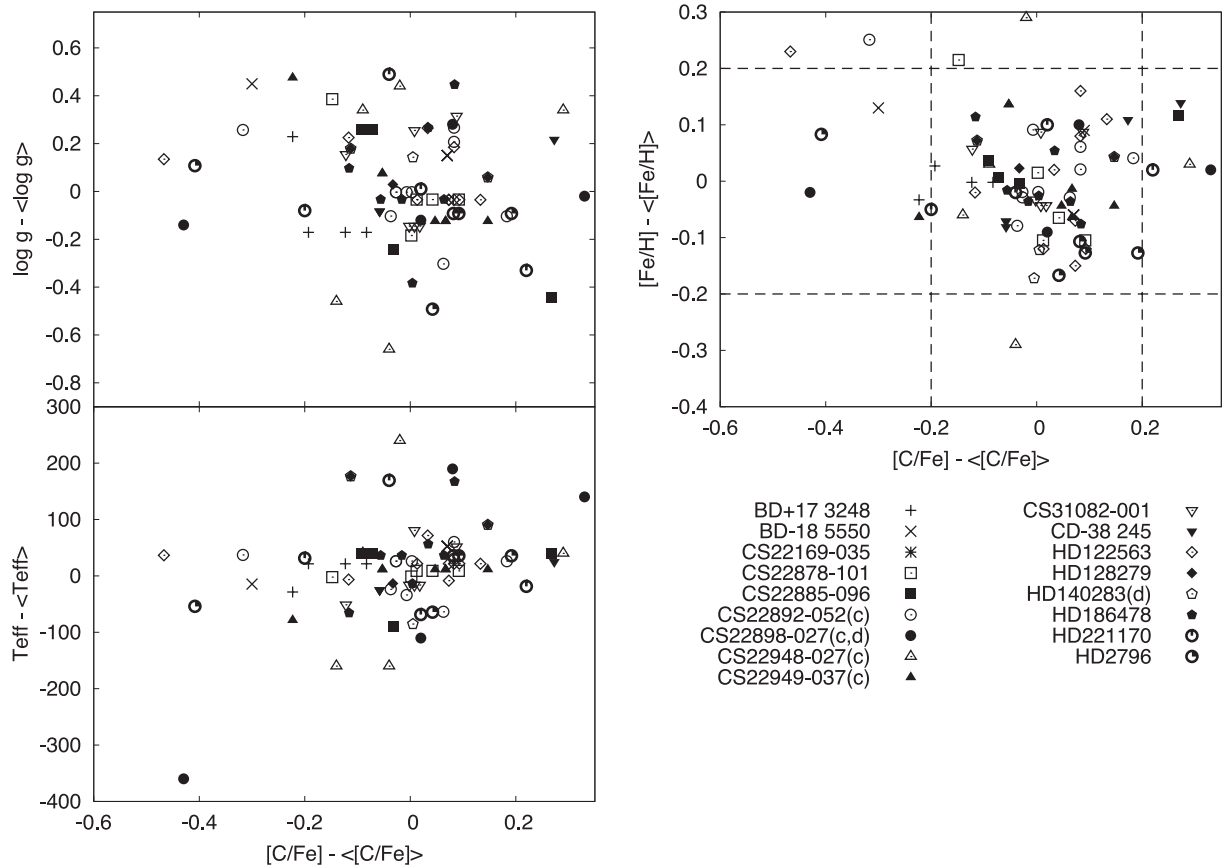
Fig. 10. Consistency check of the independent analyses for selected 17 stars from SAGA database. Each value denotes the deviation from the average value of adopted or derived quantity in each object for which it is reported. The symbol "c" and "d" in the legend of object names denotes the "carbon-rich" and "dwarf", respectively. Other stars without symbols are giants without carbon enhancement. Note that some of the papers adopt the same set of atmospheric parameters and abundances. Such data are completely overlap with each other in this figure. Note also that the data without values reported by authors do not appear in the figure, which is sometimes the case for [C/Fe]. The majority of the data points are located within the typical errors as enclosed by auxiliary dashed lines in top right panel.

derived carbon abundances. The 13 stars among them were retrieved from the sample, for which more than 8 papers report on the abundance analysis. Twelve stars among them are giants, and do not show any carbon enhancement. The remaining 4 stars were added so as to cover the various EMP stars. They are carbon-enhanced stars of giant and dwarf (CS 22948-027 and CS 22898-027, respectively), an extremely iron-poor star having [Fe/H] ~ -4 (CD-38°245), and normal giants for which the carbon abundance has been reported in more than 5 papers (CS 22169-035). In figure 10, we show the deviations from the average values of $\log g$, $T_{\rm eff}$, and [Fe/H] as a function of those of [C/Fe]. It should be noted that all of the reported carbon abundance is based on the 1D LTE model atmosphere, and that most of the analyses adopt the synthetic spectral technique using the CH G-band. The majority of plotted stars are located within 0.2 dex for the [C/Fe] value, which is well-explained in terms of the errors associated with the different values of the atmospheric parameters, and of the use of different solar abundances from paper to paper, the latter of which can be important concerning the CNO abundance. Some of the large deviations of the adopted or derived values can also be explained by analyses based on low-resolution

spectra (for example, the case of CS 22898-027), although, the reasons for different results are not necessary obvious for all cases. As can be seen in the left panels of figure 10, the large differences are highly correlated with the deviations of the adopted values of the atmospheric parameters, the latter of which is due to the different way of analyses and corrections for the determinations of the surface gravity and the effective temperature. In fact, for CS 22948-027, the largest discrepancy of atmospheric parameters and metallicity in the figure seems to be caused by both the different methods and their correction.

Accordingly, users should be warned about a possible discrepancy of independent analyses when they use combined data derived by different authors. Under any situations when using our database, users can go back to the original papers in the data retrieval system, and check any information on analyses and discussion. Any extreme case of discrepancies, if it happens, will be discussed in the latest original paper by comparing with any previous work. Therefore, we will not continue to discuss here the systematic differences between previous work for all objects and elements in the database. For abundance determinations with a non-LTE scheme or with 3D model atmospheres, their effect for extremely metal-poor

stars should also be mentioned when considering the different analyses in more detail. However, it is beyond the scope of this paper, and is discussed in other extensive papers concerning non-LTE abundances (see, e.g., Andrievsky et al. 2007) and for a 3D model atmosphere (Asplund & García Pérez 2001; Collet et al. 2007).

At present, we are planning to include information on analyses adopted by the authors, and to implement the option of choosing the LTE or NLTE abundances. On the other hand, it is desirable to improve the quality of data by creating a homogenized dataset that enables us to refine the statistical analysis of abundance trends. For users of interest, we can provide compiled data related to the equivalent width and other necessary data for their re-analysis of the sample.

We plan to continually update the SAGA database with updates as new papers reporting on a high-resolution spectroscopic follow-up appearing in the literature. We also plan to continue an effort to provide more complete coverage of existing data, by supplementing the SAGA database with stars of higher metallicity, and by extending the temporal coverage to circa 1990. In forthcoming papers, we plan to use the updated SAGA database to more thoroughly discuss the abundance trends of EMP stars, and to compare them with theoretical models.

Note added in proof (2008 August 22):

If this is the case, object names are unified into an unique name. Users of the SAGA database are cautioned that the object names registered in the database can be different from those in the original papers. In order to avoid confusion, we put comments on the existence of multiple names in the database, as provided by the script that analyzes the SIMBAD database.

References

Andrievsky, S. M., Spite, M., Korotin, S. A., Spite, F., Bonifacio, P., Cayrel, R., Hill, V., & François, P. 2007, A&A, 464, 1081

Aoki, W., Beers, T. C., Christlieb, N., Norris, J. E., Ryan, S. G., & Tsangarides, S. 2007, ApJ, 655, 492

Aoki, W., et al. 2005, ApJ, 632, 611

Aoki, W., Ryan, S. G., Norris, J. E., Beers, T. C., Ando, H., & Tsangarides, S. 2002, ApJ, 580, 1149

Asplund, M., & García Pérez, A. E. 2001, A&A, 372, 601

Asplund, M., Lambert, D. L., Nissen, P. E., Primas, F., & Smith, V. V. 2006, ApJ, 644, 229

Barklem, P. S., et al. 2005, A&A, 439, 129

Beers, T. C., Allende Prieto, C., Wilhelm, R., Yanny, B., & Newberg, H. 2004, Publ. Astron. Soc. Aust., 21, 207

Beers, T. C., & Christlieb, N. 2005, ARA&A, 43, 531

Beers, T. C., et al. 2005, in IAU Symp. 228, From Lithium to Uranium: Elemental Tracers of Early Cosmic Evolution, ed. V. Hill, P. François, & F. Primas (Cambridge: Cambridge Univ. Press), 175

Beers, T. C., Preston, G. W., & Shectman, S. A. 1985, AJ, 90, 2089

Beers, T. C., Preston, G. W., & Shectman, S. A. 1992, AJ, 103, 1987

Bond, H. E. 1980, ApJS, 44, 517

Burris, D. L., Pilachowski, C. A., Armandroff, T. E., Sneden, C., Cowan, J. J., & Roe, H. 2000, ApJ, 544, 302

Carney, B. W., Latham, D. W., Laird, J. B., & Aguilar, L. A. 1994, AJ, 107, 2240

Carney, B. W., & Peterson, R. C. 1981, ApJ, 245, 238

Carollo, D., et al. 2007, Nature, 450, 1020

Carretta, E., Gratton, R., Cohen, J. G., Beers, T. C., & Christlieb, N. 2002, AJ, 124, 481

Cayrel, R., et al. 2004, A&A, 416, 1117

Christlieb, N., Green, P. J., Wisotzki, L., & Reimers, D. 2001a, A&A, 375, 366

Christlieb, N., Schörck, T., Frebel, A., Beers, T. C., Wisotzki, L., & Reimers, D. 2008, A&A, 484, 721

Christlieb, N., Wisotzki, L., Reimers, D., Homeier, D., Koester, D., & Heber, U. 2001b, A&A, 366, 898

Cohen, J. G., Christlieb, N., Beers, T. C., Gratton, R., & Carretta, E. 2002, AJ, 124, 470

Cohen, J. G., et al. 2004, ApJ, 612, 1107

Cohen, J. G., et al. 2006, AJ, 132, 137

Collet, R., Asplund, M., & Trampedach, R. 2007, A&A, 469, 687

François, P., et al. 2007, A&A, 476, 935

Frebel, A., et al. 2006, ApJ, 652, 1585

Frebel, A., Christlieb, N., Norris, J. E., Thom, C., Beers, T. C., & Rhee, J. 2007, ApJ, 660, L117

Fujimoto, M. Y., Ikeda, Y., & Iben I., Jr. 2000, ApJ, 529, L25

Fulbright, J. P. 2000, AJ, 120, 1841

García Pérez, A. E., & Primas, F. 2006, A&A, 447, 299

Gass, H., Liebert, J., & Wehrse, R. 1988, A&A, 189, 194

Gilroy, K. K., Sneden, C., Pilachowski, C. A., & Cowan, J. J. 1988, ApJ, 327, 298

Grevesse, N., Noels, A., & Sauval, A. J. 1996, in ASP Conf. Ser., 99, Cosmic Abundances, ed. S. S. Holt & G. Sonneborn (San Francisco: ASP), 117

Hill, V., et al. 2002, A&A, 387, 560

Hobbs, L. M., & Thorburn, J. A. 1994, ApJ, 428, L25

Honda, S., Aoki, W., Kajino, T., Ando, H., Beers, T. C., Izumiura, H., Sadakane, K., & Takada-Hidai, M. 2004, ApJ, 607, 474

Johnson, J. A. 2002, ApJS, 139, 219

Jonsell, K., Edvardsson, B., Gustafsson, B., Magain, P., Nissen, P. E., & Asplund, M. 2005, A&A, 440, 321

Komiya, Y., Suda, T., Minaguchi, H., Shigeyama, T., Aoki, W., & Fujimoto, M. Y. 2007, ApJ, 658, 367

Lucatello, S., Beers, T. C., Christlieb, N., Barklem, P. S., Rossi, S., Marsteller, B., Sivarani, T., & Lee, Y. S. 2006, ApJ, 652, L37

Masseron, T., et al. 2006, A&A, 455, 1059

Mathews, G. J., & Cowan, J. J. 1990, Nature, 345, 491

McWilliam, A., Preston, G. W., Sneden, C., & Searle, L. 1995, AJ, 109, 2757

Mishenina, T. V., & Kovtyukh, V. V. 2001, A&A, 370, 951

Nissen, P. E., Primas, F., Asplund, M., & Lambert, D. L. 2002, A&A, 390, 235

Norris, J. E., Christlieb, N., Korn, A. J., Eriksson, K., Bessell, M. S., Beers, T. C., Wisotzki, L., & Reimers, D. 2007, ApJ, 670, 774

Nouri, A., et al. 2002, J. Nucl. Sci. Technol. Suppl., 2, 1480

Otuka, N., et al. 2005, in AIP Conf. Ser. 769, International Conference on Nuclear Data for Science and Technology, ed. R. C. Haight, M. B. Chadwick, T. Kawano, & P. Talou, 561

Otsuka, N., Noto, H., Ohnishi, A., & Kato, K. 2002, Report on the IAEA Technical Meeting on Network of Nuclear Reaction Data Centres, ed. V. G. Pronyaev, O. Schwerer, & A. L. Nichols (Vienna: IAEA Nuclear Data Section), 144

Plez, B., & Cohen, J. G. 2005, A&A, 434, 1117

Preston, G. W., & Sneden, C. 2000, AJ, 120, 1014

Pritychenko, B., et al. 2006, Annals of Nuclear Energy, 33, 390

Pronyaev, V. G., Schwerer, O., & Nichols, A. L. 2002, Development of Web Editor for Charged-Particle Nuclear Reaction Data, Intern. Nuc. Data Commit. Rep. INDC(NDS)-434, (Vienna: IAEA Nuclear Data Section)

Rossi, S., Beers, T. C., & Sneden, C. 1999, in ASP Conf. Ser. 165, The Third Stromlo Symposium: The Galactic Halo, ed. B. K. Gibson, T. S. Axelrod, & M. E. Putman (San Francisco: ASP), 264

Ryan, S. G., Norris, J. E., & Beers, T. C. 1996, ApJ, 471, 254

Ryan, S. G., Norris, J. E., & Bessell, M. S. 1991, AJ, 102, 303

Simmerer, J., Sneden, C., Cowan, J. J., Collier, J., Woolf, V. M., & Lawler, J. E. 2004, ApJ, 617, 1091

Smith, V. V., Lambert, D. L., & Nissen, P. E. 1993, ApJ, 408, 262

Sneden, C., McWilliam, A., Preston, G. W., Cowan, J. J., Burris, D. L., & Armosky, B. J. 1996, ApJ, 467, 819

Sneden, C., Preston, G. W., McWilliam, A., & Searle, L. 1994, ApJ, 431, L27

Spite, M., et al. 2005, A&A, 430, 655

Suda, T., Aikawa, M., Machida, M. N., Fujimoto, M. Y., & Iben, I., Jr., 2004, ApJ, 611, 476

Suda, T., Otuka, N., Korennov, S., Yamda, S., Katsuta, Y., Ohnishi, A., Katō, K., & Fujimoto, M. Y. 2006, in 2005 Symposium on Nuclear Data, ed. Y. Tahara & T. Fukahori, Vol. INDC(JPN)-196/U, 175

Truran, J. W. 1981, A&A, 97, 391

Wanajo, S., Itoh, N., Ishimaru, Y., Nozawa, S., & Beers, T. C. 2002, ApJ, 577, 853

Zhao, G., Chen, Y.-Q., Shi, J.-R., Liang, Y.-C., Hou, J.-L., Chen, L., Zhang, H.-W., & Li, A.-G. 2006, Chin. J. Astron. Astrophys., 6, 265